

# Exotic spin, charge and pairing correlations of the two-dimensional doped Hubbard model: A symmetry-entangled mean-field approach

O. Juillet<sup>1</sup> and R. Frésard<sup>2</sup><sup>1</sup>Laboratoire LPC Caen, ENSICAEN, Université de Caen, CNRS/IN2P3, 6 Boulevard Maréchal Juin, 14050 Caen Cedex, France<sup>2</sup>Laboratoire CRISMAT, UMR CNRS-ENSICAEN 6508, 6 Boulevard Maréchal Juin, 14050 Caen Cedex, France

(Received 15 October 2012; published 25 March 2013)

Intertwining of spin, charge, and pairing correlations in the repulsive two-dimensional Hubbard model is shown through unrestricted variational calculations, with projected wave functions free of symmetry breaking. A crossover from incommensurate antiferromagnetism to stripe order naturally emerges in the hole-doped region when increasing the on-site coupling. Although effective attractive pairing interactions are identified, they are strongly fragmented in several modes including  $d$ -wave pairing and more exotic channels related to an underlying stripe. We demonstrate that the entanglement of a mean-field wave function by symmetry restoration can largely account for interaction effects, and that our approach is exact for a two-site cluster.

DOI: [10.1103/PhysRevB.87.115136](https://doi.org/10.1103/PhysRevB.87.115136)

PACS number(s): 71.10.Fd, 02.60.Pn, 03.75.Ss, 74.20.Rp

Transition metal oxides are prototypical strongly correlated systems that exhibit a rich variety of quantum phenomena such as antiferromagnetism (AF), incommensurate charge and spin ordering, or high- $T_c$  superconductivity. The understanding of their subtle competition at low-temperature remains one of the most challenging topics in condensed matter physics. According to Anderson's proposal,<sup>1</sup> the two-dimensional (2D) single-band Hubbard model is expected to provide a minimal framework for addressing these issues in rare-earth cuprates. It describes  $d$  electrons hopping between the Wannier states of neighboring lattice sites in a copper-oxygen plane experiencing a purely local Coulomb repulsion. At half filling, the interaction strength drives a Mott transition to an insulator<sup>2</sup> with long-ranged AF order.<sup>3</sup> When the lattice is doped away from half filling, the exact form of the phase diagram is still controversial. Of central interest in this regime is whether the ground state supports unconventional fermion-pair condensates or charge inhomogeneities and, if so, how their order parameters are intertwined with magnetic properties. Only a partial answer can be currently obtained through approximate many-body techniques, such as cluster extensions<sup>4,5</sup> of the dynamical mean-field theory,<sup>5,6</sup> the two-particle self-consistent approximation,<sup>5,7</sup> Gutzwiller variational schemes,<sup>5,8</sup> or slave-boson approaches.<sup>5,9,10</sup> Standard quantum Monte Carlo simulations (QMC) are also restricted<sup>11</sup> owing to the notorious sign problem that is particularly severe for doped Hubbard models. Although new sign-free stochastic reformulations have been recently introduced,<sup>12,13</sup> they are not, for now, immune to systematic errors.<sup>14</sup> To overcome these theoretical difficulties, a direct quantum simulation has been suggested by loading ultracold mixtures of two interacting fermionic species into optical lattices. Indeed, such atomic systems allow for an almost perfect implementation of the Hubbard model with tunable parameters.<sup>15</sup> The crossover from a metallic into a Mott-insulating regime has already been observed,<sup>16</sup> while magnetic ordering and potential exotic superfluidity remains to be achieved using, e.g., new cooling techniques.<sup>17</sup>

Most variational investigations of low-lying states in the Hubbard model are carried out starting from a simple mean-field wave function to include quantum correlation effects

through projection techniques. For instance, the celebrated Gutzwiller ansatz suppresses (totally or partially) double occupancy in the strong-correlation regime from a  $d$ -wave superconducting state<sup>18</sup> or from a Slater determinant with assumed magnetic and charge orders.<sup>18,19</sup> Such a procedure substitutes for an unrestricted calculation, which is currently numerically intractable but highly desirable to identify the low-energy orders that spontaneously emerge from the 2D Hubbard model. The purpose of this paper is to extract spin, charge, and pairing correlations that result from an unbiased energy minimization using an alternative projected wave function.

The single-band Hubbard Hamiltonian on a  $D$ -dimensional lattice with periodic boundary conditions may be written as

$$\hat{H} = -t \sum_{\langle \vec{r}, \vec{r}' \rangle \sigma} \hat{c}_{\vec{r}\sigma}^\dagger \hat{c}_{\vec{r}'\sigma} + U \sum_{\vec{r}} \hat{n}_{\vec{r}\uparrow} \hat{n}_{\vec{r}\downarrow}, \quad (1)$$

where  $t$  is the hopping integral between neighboring sites  $\langle \vec{r}, \vec{r}' \rangle$  and  $U$  is the local Coulomb interaction;  $\hat{c}_{\vec{r}\sigma}^\dagger$ ,  $\hat{c}_{\vec{r}\sigma}$ , and  $\hat{n}_{\vec{r}\sigma} = \hat{c}_{\vec{r}\sigma}^\dagger \hat{c}_{\vec{r}\sigma}$  are, respectively, electronic creation, annihilation and density operators at site  $\vec{r}$  with spin label  $\sigma \in \{\uparrow, \downarrow\}$ . To describe the lowest-energy  $N$ -electron eigenstate for given quantum numbers  $\Gamma$ , the variational approach we propose relies on a trial Slater determinant  $|\Phi\rangle = \hat{c}_{\phi_1}^\dagger \cdots \hat{c}_{\phi_N}^\dagger |0\rangle$  projected on the symmetry subspace associated to  $\Gamma$ . Here,  $\hat{c}_{\phi_n}^\dagger = \sum_{\vec{r}\sigma} \hat{c}_{\vec{r}\sigma}^\dagger \phi_n(\vec{r}\sigma)$  creates one electron in the spinor wave function  $\phi_n(\vec{r}\sigma)$ . These single-particle states are constrained to be normalized and orthogonal, i.e.,  $\langle \phi_n | \phi_{n'} \rangle = \delta_{n,n'}$ . For the Hubbard model (1),  $\Gamma$  quantum numbers include total pseudomomentum  $\hbar \vec{K}$ , total spin  $S$ , and its  $z$  component  $S_z$ , as well as labels associated with discrete lattice symmetries. In the language of group theory,  $\Gamma$  defines an irreducible representation of the Hamiltonian symmetry group. A symmetry-adapted mean-field state  $|\Psi^{(\Gamma)}\rangle = \hat{P}^{(\Gamma)} |\Phi\rangle$  can thus be obtained by applying the standard projection operator  $\hat{P}^{(\Gamma)}$  given by<sup>20</sup>

$$\hat{P}^{(\Gamma)} = \frac{d^{(\Gamma)}}{\Omega} \sum_g (\chi_g^{(\Gamma)})^* \hat{U}_g, \quad (2)$$

where the sum runs over all symmetry transformations  $g$  realized by unitary operators  $\hat{U}_g$  in the many-body Hilbert

space. The set  $\{\chi_g^{(\Gamma)}\}$  corresponds to the character of the representation  $\Gamma$  and  $d^{(\Gamma)}$  to its dimension.  $\Omega = \sum_g 1$  is the order of the symmetry group. In the case of continuous transformations, the sum has to be supplemented by group integration with the Haar measure.<sup>20</sup> For instance, SU(2) spin-rotational symmetry restoration can be performed using Euler's angles  $(\alpha, \beta, \gamma)$  parametrization of rotations, i.e.,  $\hat{U}_g = \exp(-i\alpha\hat{S}_z/\hbar)\exp(-i\beta\hat{S}_y/\hbar)\exp(-i\gamma\hat{S}_z/\hbar)$  with  $\hat{S}$  being the total spin observable. The projection property  $(\hat{P}^{(\Gamma)})^2 = \hat{P}^{(\Gamma)}$  and the Hamiltonian invariance under the symmetry group transformations  $\hat{U}_g$  allow us to cast the average energy  $E^{(\Gamma)}$  in the projected state  $|\Psi^{(\Gamma)}\rangle$  in the form

$$E^{(\Gamma)} = \frac{\langle \Phi | \hat{H} \hat{P}^{(\Gamma)} | \Phi \rangle}{\langle \Phi | \hat{P}^{(\Gamma)} | \Phi \rangle}. \quad (3)$$

Symmetry-restored wave functions are usually considered by applying the quantum number projection (2) on top of a Hartree-Fock mean-field state.<sup>21</sup> However, such a procedure leads only to a slight improvement of the energy. Here, we follow an alternative strategy through a direct optimization of the reference state  $|\Phi\rangle$  to minimize the projected energy (3). In this way, the state  $|\Phi\rangle$  is not a solution of usual Hartree-Fock equations but corresponds to a stationary point for the energy only after projection. Furthermore, the variational ansatz is no longer a single Slater determinant but a linear superposition of product states that can absorb electronic correlations beyond mean-field. The crucial difference between symmetry projections after or before variation of the reference state  $|\Phi\rangle$  can simply be demonstrated by considering the two-site  $\vec{r}_a, \vec{r}_b$  repulsive Hubbard model at half filling. By parametrizing single-particle states of the Slater determinant  $|\Phi\rangle$  according to  $\hat{c}_{\phi_1}^\dagger = \cos(\theta/2)\hat{c}_{\vec{r}_a\uparrow}^\dagger + \sin(\theta/2)\hat{c}_{\vec{r}_b\uparrow}^\dagger$  and  $\hat{c}_{\phi_2}^\dagger = \sin(\theta/2)\hat{c}_{\vec{r}_a\downarrow}^\dagger + \cos(\theta/2)\hat{c}_{\vec{r}_b\downarrow}^\dagger$ , the projected energy (3) in the spin-singlet subspace reads  $E^{(S=0)} = (U \sin^2 \theta - 4t \sin \theta)/(1 + \sin^2 \theta)$ . The Hartree-Fock solution ( $\theta = \pi/2$  if  $U \leq 2t$  and  $\sin \theta = 2t/U$  otherwise) does not correspond to the absolute minimum of  $E^{(S=0)}$ . It is obtained for  $\sin \theta = (\sqrt{U^2 + 16t^2} - U)/(4t)$  in which case the exact ground-state energy and wave function are recovered. In this toy model, the spin projection before variation of the reference state  $|\Phi\rangle$  thus yields the exact result at *any* coupling  $U > 0$ .

In the general case, the expectation values of the many-body operators  $\hat{H} \hat{P}^{(\Gamma)}$  and  $\hat{P}^{(\Gamma)}$  in the Slater determinant  $|\Phi\rangle$  are only expressed, from Wick's theorem, in terms of the contractions  $\rho_{\vec{r}\sigma, \vec{r}'\sigma'} = \langle \hat{c}_{\vec{r}\sigma}^\dagger \hat{c}_{\vec{r}'\sigma'} \rangle_\Phi = \sum_n \phi_n(\vec{r}\sigma) \phi_n^*(\vec{r}'\sigma')$ . Therefore, the projected energy (3) is a functional of  $\rho$ :  $E^{(\Gamma)} = E^{(\Gamma)}[\rho]$ . By introducing an  $N \times N$  Hermitian matrix of Lagrange multipliers  $\lambda_{nn'}$ , stationarity of the Lagrangian function  $E^{(\Gamma)} - \sum_{n,n'} \lambda_{nn'} \langle \phi_n | \phi_{n'} \rangle$  with respect to single-particle states immediately leads to the self-consistency equation  $[h^{(\Gamma)}, \rho] = 0$ , where  $h^{(\Gamma)}$  is an effective single-particle Hamiltonian defined by the following matrix elements:

$$h_{\vec{r}\sigma, \vec{r}'\sigma'}^{(\Gamma)} = \frac{\partial E^{(\Gamma)}}{\partial \rho_{\vec{r}'\sigma', \vec{r}\sigma}}. \quad (4)$$

These results remain obviously valid irrespective of the precise form of the operator  $\hat{P}^{(\Gamma)}$ . In the mean-field approach,  $\hat{P}^{(\Gamma)}$  is

set to identity and one recovers from Eq. (3) the usual energy functional  $E[\rho]$  and from Eq. (4) the associated single-particle Hartree-Fock Hamiltonian:

$$h[\rho] = -t \sum_{(\vec{r}, \vec{r}')\sigma} |\vec{r}\sigma\rangle \langle \vec{r}'\sigma| + U \sum_{\vec{r}\sigma} (\rho_{\vec{r}\bar{\sigma}, \vec{r}\bar{\sigma}} |\vec{r}\sigma\rangle \langle \vec{r}\sigma| - \rho_{\vec{r}\sigma, \vec{r}\bar{\sigma}} |\vec{r}\sigma\rangle \langle \vec{r}\bar{\sigma}|), \quad (5)$$

where  $\sigma$  and  $\bar{\sigma}$  are time-reversed conjugate spin states. Consequently, with or without symmetry restoration, optimal spin orbitals  $\phi_n(\vec{r}\sigma)$  are obtained as eigenvectors of the state-dependent Hamiltonian (4). A similar conclusion has been drawn previously in nuclear physics<sup>22</sup> and for molecular electronic structure.<sup>23</sup> The projected-energy derivative with respect to  $\rho$  can be further calculated by noting that the transformed state  $|\Phi_g\rangle = \hat{U}_g |\Phi\rangle$  is again a Slater determinant. Owing to the extended Wick's theorem for matrix elements,<sup>24</sup> the symmetry-entangled mean-field (SEMF) Hamiltonian (4) finally becomes

$$h^{(\Gamma)}[\rho] = \frac{1}{\sum_g (\chi_g^{(\Gamma)})^* \det A_g} \sum_g (\chi_g^{(\Gamma)})^* A_g^{-1} \times \{(U_g - 1)(E[\mathcal{R}_g] - E^{(\Gamma)}) + h[\mathcal{R}_g] U_g B_g^{-1}\}. \quad (6)$$

Here the matrices  $A_g$  and  $B_g$  depend on the one-body density  $\rho$  and on the matrix representation  $U_g$  in the one-electron space of group transformations according to

$$A_g = 1 + (U_g - 1)\rho, \quad B_g = 1 + \rho(U_g - 1). \quad (7)$$

$\mathcal{R}_g = U_g \rho A_g^{-1}$  is the transition one-body density matrix<sup>24</sup> between the uncorrelated state  $|\Phi\rangle$  and its symmetry-transformed counterpart  $|\Phi_g\rangle$ :  $(\mathcal{R}_g)_{\vec{r}\sigma, \vec{r}'\sigma'} = \langle \Phi | \hat{c}_{\vec{r}'\sigma'}^\dagger \hat{c}_{\vec{r}\sigma} | \Phi_g \rangle / \langle \Phi | \Phi_g \rangle$ . In practice, no restriction is imposed on the reference state  $|\Phi\rangle$ . In particular, the usual factorization of  $|\Phi\rangle$  into a product of up-spin and down-spin Slater determinants has turned out to be inefficient. In all following numerical applications, we allow mono-electronic states to develop spin textures in the  $x$ - $y$  plane. All symmetries of the Hamiltonian (1) are restored, that lead to a variational wave function formed by the linear superposition of about  $10^6$  symmetry-related Slater determinants for the rectangular  $16 \times 4$  cell we consider below. On small  $4 \times 4$  clusters, where Hamiltonian diagonalization can be fully performed, we show in the Supplemental Material that the ground-state energy and various correlation functions differ respectively by less than 1% and 2.5% with respect to exact results.<sup>25</sup> At half filling, where unbiased QMC calculations have been performed,<sup>11</sup> the relative error on the energy at  $U = 4t$  is 0.5% (1.5%) on the  $6 \times 6$  ( $8 \times 8$ ) lattice. In several cases, the SEMF approach outperforms the usual Gutzwiller variational scheme.

Let us now focus on magnetic and charge correlations from intermediate to strong coupling. We concentrate on a hole doping  $\delta = 1/8$  where stripe orders and nonconventional superconductivity have been reported to compete from experiments on cuprates.<sup>26</sup> Note that large cell sizes are required for the development of possible incommensurate ordering with long wavelength. To meet this challenge by means of a variational calculation with an unrestricted projected wave function, we applied the above symmetry-entangled mean-field approach

limiting ourselves to a rectangular  $16 \times 4$  cell with periodic boundary conditions. A smaller dimension in the  $x$  direction would not allow us to capture translationally invariant filled vertical stripe phases that are expected from constrained-path QMC calculations.<sup>27</sup> Only zero total pseudomomentum and spin-singlet states are addressed. These quantum numbers rigorously characterize the ground state at half filling on a square lattice.<sup>28,29</sup> They are also found for the hole-doped case in exact diagonalization<sup>30</sup> and path-integral renormalization-group studies<sup>31</sup> on small clusters. Furthermore, Nagaoka ferromagnetism, which could invalidate such a statement, is not expected for the relatively moderate values  $U \leq 12t$  of the on-site repulsion we consider. Finally, the  $A_1$  irreducible representation of the  $C_{2v}$  lattice group, which embraces  $s$ -wave and  $d$ -wave symmetries, is imposed. Since our variational state is translationally and spin-rotationally invariant, possible magnetic and charge ordering can only be highlighted through correlation functions or their Fourier transform. Hence, we calculate the spin  $S_m(\vec{k})$  and charge  $S_c(\vec{k})$  structure factors defined by

$$S_m(\vec{k}) = \frac{4}{3} \sum_{\vec{r}} \exp(i\vec{k} \cdot \vec{r}) \langle \hat{S}_0^{\dagger} \hat{S}_{\vec{r}} \rangle_{\Psi^{(U)}},$$

$$S_c(\vec{k}) = \sum_{\vec{r}} \exp(i\vec{k} \cdot \vec{r}) \langle \delta \hat{n}_0 \delta \hat{n}_{\vec{r}} \rangle_{\Psi^{(U)}},$$
(8)

where  $\hat{S}_{\vec{r}} = \frac{1}{2} \sum_{\sigma, \sigma'} \hat{c}_{\vec{r}\sigma}^{\dagger} \vec{\tau}_{\sigma, \sigma'} \hat{c}_{\vec{r}\sigma'}$  is the spin operator at lattice node  $\vec{r}$  (with  $\vec{\tau}$  being the usual Pauli matrices) and  $\delta \hat{n}_{\vec{r}} = \sum_{\sigma} (\hat{n}_{\vec{r}\sigma} - \langle \hat{n}_{\vec{r}\sigma} \rangle_{\Psi^{(U)}})$  being the local charge fluctuation. Figure 1(a) shows  $S_m(\vec{k})$  in the upper-right quarter of the first Brillouin zone for relevant parameter values. It entails two main features: First, a weakly  $\vec{k}$ -dependent broad background manifestly appears and is almost insensitive to the interaction. Second, with increasing  $U/t$ , the peak at the AF wave vector  $\vec{k} = (\pi, \pi)$  decreases (to the extent that it vanishes for  $U \geq 8t$ ) and it leaves place to incommensurate magnetic correlations signaled by the symmetry-related peaks at  $\vec{k} = (\pm 7\pi/8, \pi)$ . This physically corresponds to staggered magnetization periodically modulated with the wavelength  $\lambda_m = 16 = 2\delta$ . The crossover that may be inferred from these spin-spin correlations is further confirmed by the charge structure factor  $S_c(\vec{k})$  shown in Fig. 1(b). Indeed, for intermediate coupling  $U = 4t$ , no particular signal emerges. On the contrary, from  $U = 6t$  to  $U = 12t$ , a peak at  $\vec{k} = (\pm\pi/4, 0)$  gradually develops. It follows from the translationally invariant superposition of broken-symmetry charge-density wave states associated to a hole density profile of wavelength  $\lambda_c = 8$ . Since  $\lambda_c = \lambda_m/2$ , this is the signature of filled vertical stripes at the boundaries of AF domains separated by  $\pi$  phase shifts, in agreement with the solitonic mechanism proposed by Zaanen and Oleś.<sup>32</sup> In short, we have observed, with SEMF wave functions, the crossover predicted by constrained-path QMC<sup>27</sup> from a spin-density wave to a stripe-like state with increasing Coulomb interaction.

After having tested our projected wave functions from the energetical, magnetic, and charge points of view, we now address the development of pairing correlations. We apply Yang's criteria for off-diagonal long-ranged order.<sup>33</sup> Upon the diagonalization of a pair-field correlation matrix

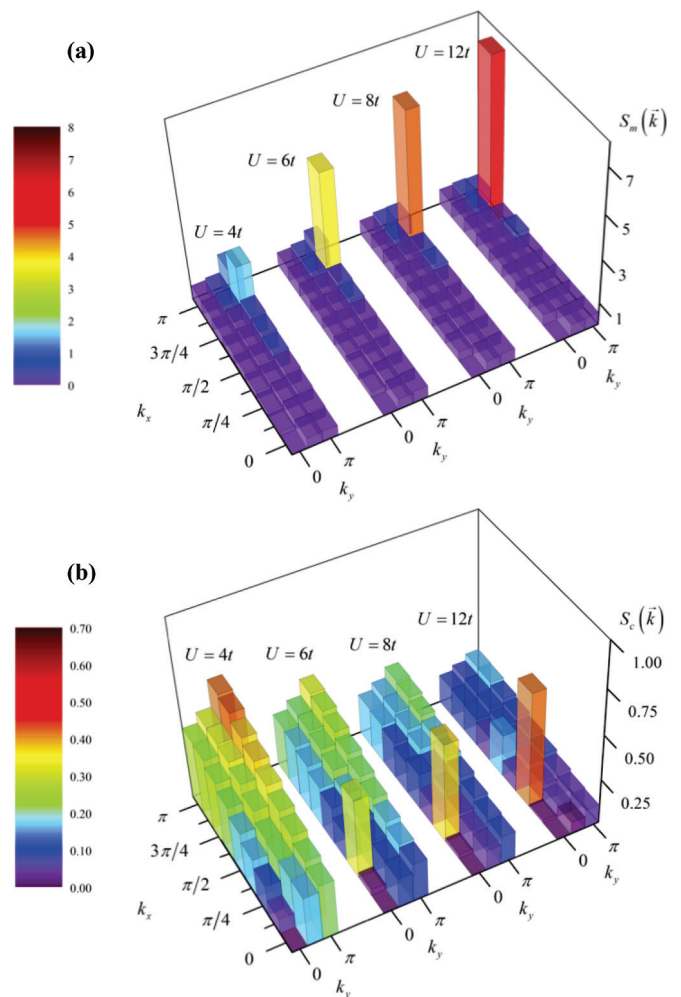


FIG. 1. (Color online) Momentum dependence of (a) magnetic and (b) charge structure factors for a rectangular  $16 \times 4$  cell at hole doping  $\delta = 1/8$  and for several values of interaction strength  $U/t$ .

$\mathcal{P}_{\vec{r}, \vec{r}'}$ , superconductivity appears as long as one or more eigenvalue scales as the particle number when the system size is increased at fixed density. The associated eigenvectors define pair wave functions. Here, we deal with a finite system and only electron pairing modes favored by the interaction may be identified. Moreover, one has to discard fictitious correlations from noninteracting dressed electrons that only vanish at the thermodynamic limit. Hence, for spin-singlet pairing, we use the following matrix  $\mathcal{P}_{\vec{r}, \vec{r}'}$ :

$$\mathcal{P}_{\vec{r}, \vec{r}'} = \frac{1}{2} \langle \hat{\Pi}_{\vec{r}}^{\dagger} \hat{\Pi}_{\vec{r}'} + \hat{\Pi}_{\vec{r}} \hat{\Pi}_{\vec{r}'}^{\dagger} \rangle_{\Psi^{(U)}}^{(V.C.)},$$
(9)

where  $\hat{\Pi}_{\vec{r}}^{\dagger} = \frac{1}{\sqrt{2N}} \sum_{\vec{R}} (\hat{c}_{\vec{R}\uparrow}^{\dagger} \hat{c}_{\vec{R}+\vec{r}\downarrow}^{\dagger} - \hat{c}_{\vec{R}\downarrow}^{\dagger} \hat{c}_{\vec{R}+\vec{r}\uparrow}^{\dagger})$  is the translationally invariant and spin-singlet pair-field operator for two electrons separated by  $\vec{r}$  and  $N$  is the number of lattice sites;  $\langle \dots \rangle^{(V.C.)}$  stands for the vertex contribution.<sup>34</sup> We display in Table I the first eigenvalues of the  $\mathcal{P}$  matrix in the strongly repulsive regime  $U = 12t$  as compared to those obtained for the attractive coupling  $U = -4t$ . In both cases, positive eigenvalues are obtained. They result purely from the entanglement realized by symmetry restoration: Without projection, the matrix elements  $\mathcal{P}_{\vec{r}, \vec{r}'}$  are all vanishing. For

TABLE I. First eigenvalues  $\lambda_i$  of pairing correlation matrix  $\mathcal{P}_{\vec{r},\vec{r}'}$  defined by Eq. (9). Results are shown for a  $16 \times 4$  cluster in an  $s$ -wave BCS-like superconducting regime ( $N = 30$  electrons,  $U = -4t$ ) and in the striped state obtained for the strong Coulomb repulsion  $U = 12t$  at hole doping  $\delta = 1/8$  ( $N = 56$  electrons).

$U/t$	$N$	$\lambda_1$	$\lambda_2$	$\lambda_3$	$\lambda_4$	$\lambda_5$
-4	30	0.421	0.051	0.046	0.030	0.020
12	56	0.495	0.455	0.442	0.431	0.425

the 2D attractive Hubbard model, off-diagonal long-ranged order associated to BCS  $s$ -wave superconductivity is well established for moderate interactions, especially in the vicinity of quarter filling.<sup>35</sup> The SEMF approach gives here good evidence for a precursor to the superconducting behavior, since one pairing eigenmode clearly outperforms the other ones. Truly, the associated pair wave function exhibits a large on-site component accompanied with a small extended- $s$  contribution. In the repulsive regime, perhaps the most striking result consists of highlighting the emergence of an effective attractive interaction in the particle-particle channel. However, it is strongly fragmented as all first few eigenvalues are nearly degenerate. Concerning the pairing symmetry, Fig. 2 presents the wave function associated to the leading modes. On top of the expected  $d$ -wave [Fig. 2(a)] and extended  $s$ -wave [Fig. 2(e)] pairing,<sup>36</sup> exotic competing modes related to stripe-like correlations are found. They are characterized

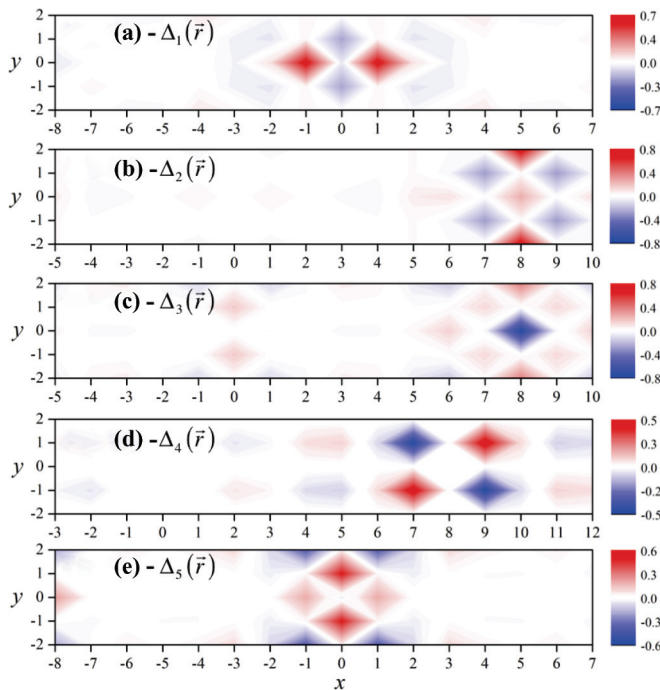


FIG. 2. (Color online) Wave functions  $\Delta_i(\vec{r})$  associated with pairing modes defined by eigenvectors of the  $\mathcal{P}$  matrix (9) with the largest eigenvalues  $\lambda_i$  shown in Fig. 2.  $\hat{\Delta}_i^\dagger = \frac{1}{\sqrt{2N}} \sum_{\vec{r},\vec{R}} \Delta_i(\vec{r}) (\hat{c}_{\vec{R}\uparrow}^\dagger \hat{c}_{\vec{R}+\vec{r}\downarrow}^\dagger - \hat{c}_{\vec{R}\downarrow}^\dagger \hat{c}_{\vec{R}+\vec{r}\uparrow}^\dagger)$  is the corresponding pair-field operator. A  $16 \times 4$  lattice with  $U = 12t$  is considered at hole doping  $\delta = 1/8$ .

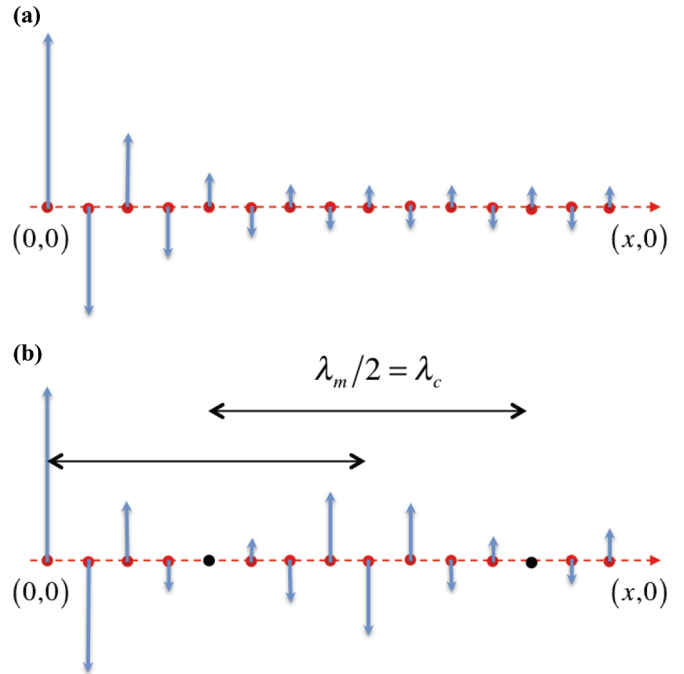


FIG. 3. (Color online) Schematic view of (a) singlet-electron pairing in a correlated AF background and (b) in presence of a domain wall associated with an underlying filled stripe. (a) The length of the individual spins mimics the decrease of the spin autocorrelation function at small distances together with its long-ranged constant-staggered magnetization. Thus, only nearest-neighbor pairing dominates. (b) With holes localized in a vertical filled stripe, the incommensurate magnetic peak implies the repetition of a similar AF spin pattern between domain walls, with a  $\pi$  phase shift at the nodes. Therefore, the formation of singlet pairs at distances  $x = \lambda_m/2 (= \lambda_c)$  is favored.

by pairing at distances close to the charge wavelength  $\lambda_c = 8$ . Qualitatively, the formation of a singlet pair in a correlated AF background can be enhanced at this distance  $\lambda_c = \lambda_m/2$  provided a domain wall separates the two electrons. This is schematically depicted in Fig. 3. No significant deviation appears when reducing  $U$  in the stripy regime. For the intermediate coupling  $U = 4t$ , where no charge order can be detected, only  $d$ -wave [Fig. 2(a)] and extended  $s$ -wave pairings are dominant.

In conclusion, we have performed unrestricted variational calculations for the 2D hole-doped Hubbard model in a theoretical framework where electronic correlations are generated by the entanglement of a mean-field wave function through the restoration of all Hamiltonian symmetries. From moderate to strong coupling, independent energy minimizations lead to consistent spin, charge, and pairing correlations at doping  $\delta = 1/8$ . The spontaneous appearance of incommensurate spin-density waves evolving into striped states is accompanied by the development of several competing pairing channels. It remains to be elucidated if one of them would dominate when enlarging the variational subspace to bring out a precursor signal to unconventional superconductivity. Work along this line is in progress.

- <sup>1</sup>P. W. Anderson, *Science* **235**, 1196 (1987).
- <sup>2</sup>F. F. Assaad and M. Imada, *Phys. Rev. Lett.* **76**, 3176 (1996).
- <sup>3</sup>J. E. Hirsch, *Phys. Rev. B* **31**, 4403 (1985).
- <sup>4</sup>T. Maier, M. Jarrell, T. Pruschke, and M. Hettler, *Rev. Mod. Phys.* **77**, 1027 (2005).
- <sup>5</sup>*Theoretical Methods for Strongly Correlated Systems*, edited by A. Avella and F. Mancini (Springer Verlag, Berlin, 2011).
- <sup>6</sup>A. Georges, G. Kotliar, W. Krauth, and M. Rozenberg, *Rev. Mod. Phys.* **68**, 13 (1996).
- <sup>7</sup>A.-M. S. Tremblay, B. Kyung, and D. Sénéchal, *Low Temp. Phys.* **32**, 424 (2006).
- <sup>8</sup>B. Edegger, V. N. Muthukumar, and C. Gros, *Adv. Phys.* **56**, 927 (2007).
- <sup>9</sup>M. Raczkowski, R. Frésard, and A. M. Oleś, *Europhys. Lett.* **76**, 128 (2006).
- <sup>10</sup>G. Seibold and J. Lorenzana, *Phys. Rev. B* **69**, 134513 (2004).
- <sup>11</sup>S. R. White, D. J. Scalapino, R. L. Sugar, E. Y. Loh, J. E. Gubernatis, and R. T. Scalettar, *Phys. Rev. B* **40**, 506 (1989).
- <sup>12</sup>J. F. Corney and P. D. Drummond, *Phys. Rev. Lett.* **93**, 260401 (2004).
- <sup>13</sup>O. Juillet, *New J. Phys.* **9**, 163 (2007).
- <sup>14</sup>P. Corboz, M. Troyer, A. Kleine, I. P. McCulloch, U. Schollwöck, and F. F. Assaad, *Phys. Rev. B* **77**, 085108 (2008).
- <sup>15</sup>W. Hofstetter, J. I. Cirac, P. Zoller, E. Demler, and M. D. Lukin, *Phys. Rev. Lett.* **89**, 220407 (2002).
- <sup>16</sup>R. Jördens, N. Strohmaier, K. Günter, H. Moritz, and T. Esslinger, *Nature (London)* **455**, 204 (2008).
- <sup>17</sup>D. C. McKay and B. De Marco, *Rep. Prog. Phys.* **74**, 054401 (2011).
- <sup>18</sup>T. Giamarchi and C. Lhuillier, *Phys. Rev. B* **42**, 10641 (1990).
- <sup>19</sup>M. Dzierzawa and R. Frésard, *Z. Phys. B* **91**, 245 (1993).
- <sup>20</sup>M. Hamermesh, *Group Theory and its Application to Physical Problems* (Addison-Wesley, Reading, MA, 1962).
- <sup>21</sup>E. Louis, F. Guinea, M. P. López Sancho, and J. A. Vergés, *Phys. Rev. B* **64**, 205108 (2001).
- <sup>22</sup>J. A. Sheikh and P. Ring, *Nucl. Phys. A* **665**, 71 (2000).
- <sup>23</sup>G. E. Scuseria, C. A. Jimenez-Hoyos, T. M. Henderson, J. K. Ellis, and K. Samanta, *J. Chem. Phys.* **135**, 124108 (2011).
- <sup>24</sup>J.-P. Blaizot and G. Ripka, *Quantum Theory of Finite Systems* (MIT Press, Cambridge, 1985).
- <sup>25</sup>See Supplemental Material at <http://link.aps.org/supplemental/10.1103/PhysRevB.87.115136> for a detailed comparison of the SEMF approach to existing data obtained by other numerical simulations.
- <sup>26</sup>N. Ichikawa, S. Uchida, J. M. Tranquada, T. Niemöller, P. M. Gehring, S.-H. Lee, and J. R. Schneider, *Phys. Rev. Lett.* **85**, 1738 (2000).
- <sup>27</sup>C.-C. Chang and S. Zhang, *Phys. Rev. Lett.* **104**, 116402 (2010).
- <sup>28</sup>E. H. Lieb, *Phys. Rev. Lett.* **62**, 1201 (1989).
- <sup>29</sup>A. Moreo and E. Dagotto, *Phys. Rev. B* **41**, 9488 (1990).
- <sup>30</sup>A. Parola, S. Sorella, M. Parrinello, and E. Tosatti, *Phys. Rev. B* **43**, 6190 (1991).
- <sup>31</sup>T. Mizusaki and M. Imada, *Phys. Rev. B* **69**, 125110 (2004).
- <sup>32</sup>J. Zaanen and A. M. Oleś, *Ann. Phys. (Berlin)* **5**, 224 (1996).
- <sup>33</sup>C. N. Yang, *Rev. Mod. Phys.* **34**, 694 (1962).
- <sup>34</sup>The quantity  $\langle \hat{c}_{r_1\sigma_1}^\dagger \hat{c}_{r_4\sigma_4} \rangle \langle \hat{c}_{r_2\sigma_2}^\dagger \hat{c}_{r_3\sigma_3} \rangle - \langle \hat{c}_{r_1\sigma_1}^\dagger \hat{c}_{r_3\sigma_3} \rangle \langle \hat{c}_{r_2\sigma_2}^\dagger \hat{c}_{r_4\sigma_4} \rangle$  is subtracted for each term of the form  $\langle \hat{c}_{r_1\sigma_1}^\dagger \hat{c}_{r_2\sigma_2}^\dagger \hat{c}_{r_3\sigma_3} \hat{c}_{r_4\sigma_4} \rangle$ .
- <sup>35</sup>M. Guerrero, G. Ortiz, and J. E. Gubernatis, *Phys. Rev. B* **62**, 600 (2000).
- <sup>36</sup>A. Moreo and D. J. Scalapino, *Phys. Rev. B* **43**, 8211 (1991).